

# Structure–Property Relations and Diffusion Pathways of the Silver Ion Conductor $\text{Ag}_5\text{Te}_2\text{Cl}$

Tom Nilges, Sara Nilges, and Arno Pfitzner\*

*Institut für Anorganische Chemie, NWF IV, Universitätsstrasse 31,  
93040 Regensburg, Germany*

Thomas Doert and Peter Böttcher†

*Institut für Anorganische Chemie, Mommsenstrasse 13, 01062 Dresden, Germany*

*Received September 22, 2003. Revised Manuscript Received November 12, 2003*

Single-crystal structure determinations at room temperature and elevated temperatures were carried out on the silver ion conductor  $\text{Ag}_5\text{Te}_2\text{Cl}$ , and the hitherto unknown structure of the room-temperature phase ( $\beta\text{-Ag}_5\text{Te}_2\text{Cl}$ ) was determined. Ion pathways are discussed for the room- and high-temperature phase by analyzing the joint probability density functions. Main transport pathways at different temperatures were worked out to obtain detailed insight into the movement of the silver atoms in this material.  $\text{Ag}_5\text{Te}_2\text{Cl}$  is an excellent 1D ionic conductor having a pronounced silver mobility along complex silver columns. Conductivities are  $\sigma = 1.51 \times 10^{-3} \Omega^{-1} \text{cm}^{-1}$  at 323 K and  $\sigma = 4.30 \times 10^{-1} \Omega^{-1} \text{cm}^{-1}$  at 469 K. With use of a nonharmonic description of the silver distribution of the high-temperature phase, a promising structure model has been derived for the room-temperature phase.  $\beta\text{-Ag}_5\text{Te}_2\text{Cl}$  can be regarded as an intermediate phase between the disordered high- and the ordered low-temperature phase, showing an almost ordered silver distribution in addition to a slightly different arrangement of the anionic substructure.

## Introduction

Most of the superionic conductors known to date are polymorphic compounds with several phase transitions and distinct ionic conductivities due to changes in the substructure of the mobile ions. Encouraged by the superionic properties of silver iodide, an enormous number of studies of ternary and quaternary compounds has been performed with the aim to stabilize superionic phases at lower temperatures.<sup>1</sup> One of the most intensely investigated systems in the field of silver ion conductivity is the system  $\text{RbI-AgI}$  including the superionic conductor  $\text{RbAg}_4\text{I}_5$ . Structural investigations of this compound were first mentioned in 1967 by Geller<sup>2</sup> and Bradley et al.<sup>3</sup> and are still in progress.<sup>4</sup> The conduction mechanism<sup>5</sup> and the preferred conduction pathways in ionic conductors (e.g., in  $\text{Ag}_7\text{PSe}_6$ )<sup>6</sup> are of special interest due to their potential technological application in solid-state batteries or electrochemical cells. The knowledge of the mechanism and the underlying structure is essential for the exploration of new optimized ion conductors.

$\text{Ag}_5\text{Te}_2\text{Cl}$  shows the typical behavior of an ion-conducting material, that is, polymorphism in combination with ion conduction in its high-temperature phase. Two modifications have been characterized structurally so far: a high-temperature  $\alpha$ -phase showing enhanced ionic conductivity in addition to highly delocalized silver atoms in the cation substructure and a low-temperature  $\gamma$ -phase with a clustered arrangement of silver on distinct positions. The crystal structure of  $\alpha\text{-Ag}_5\text{Te}_2\text{Cl}$  was first examined by Blachnik and Dreisbach in 1985.<sup>7</sup> Due to the high silver mobility, the cation substructure was described using 7, not fully occupied silver positions. According to the authors, a certain number of silver positions with low occupancy factors were omitted in their structure model. This finding, namely, numerous positions with almost equivalent potential energies, is typical for an ion conductor. Blachnik also mentioned the occurrence of a twinned room-temperature phase with a monoclinic unit cell and a monoclinic angle close to 90°. This phase,  $\beta\text{-Ag}_5\text{Te}_2\text{Cl}$ , was later found to exist between 237(2) and 329(3) K. However, the structure and physical properties of this phase were not reported so far.<sup>8</sup> The crystal structure of the third polymorph,  $\gamma\text{-Ag}_5\text{Te}_2\text{Cl}$ , which is stable below 237 K and was originally found in DSC measurements, was reported in 2000.<sup>8</sup> Electrical properties of  $\text{Ag}_5\text{Te}_2\text{Cl}$  in the temperature range of 150–400 K were reported by Beeken

\* To whom correspondence should be addressed. Phone: (+)499419434551. Fax: (+)499419434983. E-mail: arno.pfitzner@chemie.uni-regensburg.de.

† Deceased June 30, 2003.

(1) Funke, K. *Prog. Inorg. Chem.* **1976**, *11*, 345.

(2) Geller, S. *Science* **1967**, *157*, 310.

(3) Bradley, J. N.; Greene, P. D. *Trans. Faraday Soc.* **1967**, *63*, 2516.

(4) Hull, S.; Keen, D. A.; Sivia, D. S.; Berastegui, P. *J. Solid State Chem.* **2002**, *165*, 363.

(5) Funke, K. *Defect Diffus. Forum* **1997**, *143*, 1243.

(6) Evain, M.; Gaudin, E.; Boucher, F.; Petricek, V.; Taulelle, F. *Acta Crystallogr.* **1998**, *B54*, 376.

(7) Blachnik, R.; Dreisbach, H. A. *J. Solid State Chem.* **1985**, *60*, 115.

(8) Doert, Th.; Rönsch, E.; Schnieders, F.; Böttcher, P.; Sieler, J. *Z. Anorg. Allg. Chem.* **2000**, *626*, 89.

et al.<sup>9</sup>  $\alpha\text{-Ag}_5\text{Te}_2\text{Cl}$  shows a high ionic conductivity above 329 K with a conductivity of approximately  $\sigma = 10^{-1} \Omega^{-1} \text{cm}^{-1}$  and an activation energy of 0.26 eV; the activation energy for  $\beta\text{-Ag}_5\text{Te}_2\text{Cl}$  is 0.38 eV according to these authors. The activation energy for  $\alpha\text{-Ag}_5\text{Te}_2\text{Cl}$ , based on a limited number of data, is relatively high as compared to many other ion-conducting materials.<sup>10</sup>

Herein, we report the crystal structures and electrical properties of  $\beta\text{-}$  and  $\alpha\text{-Ag}_5\text{Te}_2\text{Cl}$  in the temperature range between 298 and 543 K. A so-called nonharmonic refinement of the displacement parameters of the mobile silver ions using a Gram-Charlier expansion<sup>11</sup> up to the 4th order makes it possible to improve the structure model for  $\alpha\text{-Ag}_5\text{Te}_2\text{Cl}$ . The diffusion pathways of silver ions in the three-dimensional (3D) anion network can be estimated for both phases from a detailed analysis of the joint probability density functions (jpdf).<sup>12,13</sup>

## Experimental Section

**Synthesis of  $\text{Ag}_5\text{Te}_2\text{Cl}$ .**  $\text{Ag}_5\text{Te}_2\text{Cl}$  was prepared from a 1:4:2 mixture of  $\text{AgCl}$  (Alfa 99.999%),  $\text{Ag}$  (Chempur 99.9%), and  $\text{Te}$  (Chempur 99.9%) in quartz ampoules. All starting materials were used without further purification. The mixture was heated to 753 K for 5 days. After homogenization of the crude product,  $\text{TeCl}_4$  was added as a transport agent and the mixture was heated in a two-zone oven using a vertical temperature gradient (423–453 K).  $\text{TeCl}_4$  was prepared from  $\text{Te}$  and dried  $\text{Cl}_2$ <sup>14</sup> (Messer Griesheim 99.8%) and purified by sublimation in a  $\text{Cl}_2$  stream. Single crystals with a size up to 5 mm (longest edge) were obtained.

**EDX Analysis.** Energy-dispersive X-ray analyses were performed on a Zeiss DSM 950 scanning electron microscope fitted with a ZAF-4/FLS SE-detector. Samples of  $\text{Ag}_5\text{Te}_2\text{Cl}$  were measured at room temperature. Five different crystals were examined to give an average composition of  $\text{Ag}_{4.94(3)}\text{Te}_{2.05(5)}\text{Cl}_{1.01(8)}$ .

**Thermal Analysis.** Difference calorimetric measurements were performed on a SETARAM DSC 111 under a  $\text{N}_2$  atmosphere in Al crucibles. A sample of ground single crystals (138.17 mg) was measured in the temperature range of 178–373 K with heating rates of 5 and 10 K/min, respectively.  $\text{Ag}_5\text{Te}_2\text{Cl}$  shows two reversible endothermic effects at 240.9(2) and 334.2(5) K, which are assigned to the  $\gamma\text{-}\beta$  and  $\beta\text{-}\alpha$  phase transition. The corresponding transition enthalpies are 1.2(1) and 11.7(1) J/g, respectively. These data are in good agreement with the data reported earlier.<sup>8,9</sup>

**Powder Diffraction Analysis.** X-ray powder measurements were carried out with ground single crystals of  $\text{Ag}_5\text{Te}_2\text{Cl}$  using a Stoe STADI P diffractometer (transmission setup, germanium monochromator,  $\text{Cu K}\alpha_1$ ,  $\lambda = 1.54051 \text{ \AA}$ , silicon as external standard) fitted with a  $5^\circ$  linear PSD. Room-temperature data were recorded from flat samples; the respective data are given in the Supporting Information. For temperature-dependent powder diffraction, an Oxford Cryosystem 600 cooling device was attached to the diffractometer, which allows one to operate at temperatures up to 370 K. The samples were filled in capillaries and data were recorded every 2 K from 220 to 350 K in the  $2\theta$  range of  $12\text{--}48^\circ$ . While the  $\gamma\text{-}\beta$  transformation cannot be detected in the powder pattern, a significant change of intensities and position of the reflections is observable at 334 K (see Figure S1, Supporting Information). This effect comes along with the thermal effect

at the same temperature and underlines the assignment of a solid–solid phase transition.

**Single-Crystal Structure Analysis.** Crystals of  $0.28 \times 0.24 \times 0.18 \text{ mm}^3$  and of  $0.41 \times 0.20 \times 0.20 \text{ mm}^3$  size were selected for data collection. Intensities were recorded on a STOE IPDS I at 298(1), 373(1), and 423(1) K (crystal 1), and on a STOE IPDS II at 298(1) and 543(1) K (crystal 2). Both diffractometers operate with  $\text{Mo K}\alpha$  radiation ( $\lambda = 0.71073 \text{ \AA}$ , graphite monochromator), and the temperature was controlled by the respective STOE heating devices. The intensities of  $\beta\text{-Ag}_5\text{Te}_2\text{Cl}$  (298 K data, crystal 1) were first averaged in the Laue group  $mmm$  and the possible space groups  $Pnma$  and  $Pna2_1$  were chosen for structure determination. No proper structure model could be obtained after structure solution<sup>16</sup> neither by direct methods nor by Patterson methods. Taking the symmetry relations between the high- and low-temperature phase into account (see Supporting Information), a symmetry reduction from  $I4/mcm$  (No. 140), the space group of  $\alpha\text{-Ag}_5\text{Te}_2\text{Cl}$ , to the monoclinic space group  $P2_1/n$  (No. 14) was deduced. A monoclinic unit cell with lattice parameters of  $a = 13.852(3) \text{ \AA}$ ,  $b = 7.663(2) \text{ \AA}$ ,  $c = 13.661(3) \text{ \AA}$ , and  $\beta = 90.09(1)^\circ$  was calculated from the respective powder diffraction data. The structure model of the high-temperature phase was then transformed into a corresponding one in  $P2_1/n$  and the refinement “converged” at  $R = 0.3299$  and  $wR = 0.4832$  (for reflections  $I_0 > 3\sigma_I$ ) after anisotropic treatment of all atoms. High residual electron density close to the heaviest atoms, unusual high displacement parameters, and the monoclinic angle of  $\beta = 90.09^\circ$  led to the conclusion that twinning occurred during the high-temperature–room-temperature phase transition to form pseudo merohedrally twinned crystals. A twin law (0 0 1, 0 1 0, 1 0 0) was thus introduced into the refinement, which significantly improved the structure model ( $R = 0.0661$  and  $wR = 0.1390$  for reflections  $I_0 > 3\sigma_I$ ). Some of the silver positions showing high and anisotropic displacement parameters were then refined using a nonharmonic approach based on a Gram Charlier expansion<sup>11</sup> with nonharmonic displacement parameters up to the 4th order. Only the significant displacement parameters ( $3\sigma$  cutoff) were refined.<sup>17</sup> During the structure investigation of numerous crystals, we found that the quality of crystals from one reaction batch can differ markedly and has thus a strong impact on the quality of the structure refinement. We achieved the best result by choosing a suitable crystal, heating to temperatures above the  $\alpha\text{-}\beta$  phase transition, and cooling to the stability area of the  $\beta$  modification directly on the diffractometer.

Intensities of  $\alpha\text{-Ag}_5\text{Te}_2\text{Cl}$  (373, 423, and 543 K data) were averaged in the Laue group  $4/mmm$  and the space group  $I4/mcm$  (No. 140) was assigned from the reflection conditions. During the refinements the sum of the occupancy factors of all silver positions was restricted to the stoichiometric value of five silver atoms per formula unit, in good agreement with the quantitative EDX measurements. After a nonharmonic treatment of the silver ion distribution comparable to the one in the room-temperature phase, a thorough analysis of the jpdf was carried out from which the preferred ionic diffusion pathways were estimated. A detailed description of a structure refinement strategy using a nonharmonic approach was discussed earlier.<sup>18,19</sup> Further details of the structure determination, atomic positions, interatomic distances, and anisotropic displacement parameters are summarized in Tables 1 and S2–S6 (Supporting Information). The maxima of probability density, the so-called mode positions, were determined from the probability density functions of all nonharmonically refined positions (Table S3, Supporting Information).

(15) Becker, P. J.; Coppens, P. *Acta Crystallogr.* **1974**, *A30*, 129.

(16) Sheldrick, G. *SHELX97, Program for the solution and refinement of crystal structures*; University of Göttingen: Göttingen, Germany, 1997.

(17) Petricek, V.; Dusek, M. *The crystallographic computing system JANA2000*; Institute of Physics: Praha, Czech Republic, 2000.

(18) Pfitzner, A.; Evain, M.; Petricek, V. *Acta Crystallogr.* **1997**, *B53*, 337.

(19) Nilges, T.; Reiser, S.; Hong, J. H.; Gaudin, E.; Pfitzner, A. *Phys. Chem. Chem. Phys.* **2002**, *4*, 5888.

(9) Beeken, R. B.; Wang S. M.; Smith D. R. *Solid State Ionics* **1992**, *53–56*, 220.

(10) Agrawal, R. C.; Gupta, R. K. *J. Mater. Sci.* **1999**, *34*, 1131.

(11) Zucker, U. H.; Schulz, H. *Acta Crystallogr.* **1982**, *A38*, 563.

(12) Willis, B. M. T. *Acta Crystallogr.* **1969**, *A25*, 277.

(13) Bachmann, R.; Schulz, H. *Acta Crystallogr.* **1984**, *A40*, 668.

(14) Braver, G. *Handbuch der Präparativen Anorganischen Chemie*; F. Enke Verlag: Stuttgart, 1975; Vol. 1, p 432.

Table 1. Crystallographic and Refinement Data for  $\alpha$ -Ag<sub>5</sub>Te<sub>2</sub>Cl and  $\beta$ -Ag<sub>5</sub>Te<sub>2</sub>Cl

empirical formula formula weight temperature	Ag <sub>5</sub> Te <sub>2</sub> Cl 830.0 g mol <sup>-1</sup>					
	298 K crystal 1	298 K crystal 2	373 K crystal 1 0.71073 Å	423 K crystal 1	543 K crystal 2	
wavelength						
crystal system	monoclinic	monoclinic	tetragonal	tetragonal	tetragonal	
phase	$\beta$	$\beta$	$\alpha$	$\alpha$	$\alpha$	
space group	$P2_1/n$ (No. 14)	$P2_1/n$ (No. 14)	$I4/mcm$ (No. 140)	$I4/mcm$ (No. 140)	$I4/mcm$ (No. 140)	
unit cell dimensions	$a$ (Å) $b$ (Å) $c$ (Å) $\beta$ (deg) (Å <sup>3</sup> )	13.852(3) <sup>a</sup> 7.663(2) <sup>a</sup> 13.661(3) <sup>a</sup> 90.09(1) <sup>a</sup> 1450.1(6)	13.852(3)* 7.663(2) <sup>a</sup> 13.661(3) <sup>a</sup> 90.09(1) <sup>a</sup> 1450.1(6)	9.747(1) 9.747(1) 7.842(1) 7.866(1)	9.778(1) 9.778(1) 7.866(1)	9.809(2) 9.809(2) 7.894(2)
volume	$Z$	8	8	4	4	
density $\rho$ (calculated)	(g cm <sup>3</sup> )	7.601	7.601	7.398(2)	7.328(2)	7.257(3)
absorption coefficient $\mu$	(mm <sup>-1</sup> )	21.41	21.41	20.83	20.64	20.44
$F(000)$		2848	2848	1424	1424	1424
crystal size	(mm)	0.28	0.41	0.28	0.28	0.41
	(mm)	0.24	0.20	0.24	0.24	0.20
	(mm)	0.18	0.20	0.18	0.18	0.20
$\theta$ range min./max.	(deg)	2.40/30.17	3.04/26.78	2.96/30.07	4.17/31.48	2.94/35.14
index range		-19 ≤ $h$ ≤ 19 -10 ≤ $k$ ≤ 10 -19 ≤ $l$ ≤ 19	-17 ≤ $h$ ≤ 17 -9 ≤ $k$ ≤ 9 -17 ≤ $l$ ≤ 17	-13 ≤ $h$ ≤ 13 -13 ≤ $k$ ≤ 13 -17 ≤ $l$ ≤ 10	-13 ≤ $h$ ≤ 14 -14 ≤ $k$ ≤ 14 -10 ≤ $l$ ≤ 11	-15 ≤ $h$ ≤ 12 -6 ≤ $k$ ≤ 15 -9 ≤ $l$ ≤ 12
type of diffractometer		IPDS I	IPDS II	IPDS I	IPDS I	IPDS II
reflections collected		18723	10484	3810	3785	1793
independent reflections		4232	2978	301	345	453
$R(\text{int})$		0.0762	0.0319	0.0416	0.0590	0.0411
completeness to $\theta$		0.983	0.958	0.997	0.986	0.994
absorption correction		numerical	numerical	numerical	numerical	numerical
max. transmission		0.1150	0.1618	0.0901	0.0872	0.1331
min. transmission		0.0442	0.0493	0.0311	0.0316	0.0260
refinement method		full matrix least squares on $F^2$ , Gram Charlier nonharmonic exp.				
twin fractions		2	2			
twin volumes		0.510(1) 0.490(1)	0.555(1) 0.444(1)			
parameters		221	224	51	50	50
goodness of fit on $F^2$		1.58	1.94	1.60	1.51	1.64
final $R$ values [ $I > 3\sigma_I$ ]	$R, x$	0.0431, 3	0.0311, 3	0.0291, 2	0.0332, 2	0.0379, 2
	$wR$	0.0840	0.0765	0.0530	0.0604	0.0733
final $R$ values [all]	$R$	0.0539	0.0346	0.0442	0.0507	0.0591
	$wR$	0.0866	0.0826	0.0554	0.0630	0.0796
extinction method			B-C type 1 Lorentzian isotropic <sup>15</sup>			
extinction coefficient		0.017(3)	none	0.35(2)	0.29(3)	0.33(2)
largest difference	(e Å <sup>-3</sup> )	1.73	1.52	0.60	0.64	0.76
peak and hole		-2.18	-1.30	-0.62	-0.51	-0.58

<sup>a</sup> Lattice constants from powder diffraction measurements.

**Conductivity Measurements.** Impedance spectra of Ag<sub>5</sub>Te<sub>2</sub>Cl were recorded with a Zahner IM6 impedance analyzer and a homemade measuring cell.<sup>20</sup> Cold pressed pellets of finely ground samples were connected to gold electrodes and platinum wires. After an equilibration time of 30 min, impedance spectra (100 mHz to 4 MHz) were recorded in a temperature range from 302 to 469 K. The samples were kept under an oxygen and moisture free argon atmosphere during the measurements.

## Results and Discussion

**Structure Description.** Starting from the high-temperature modification of Ag<sub>5</sub>Te<sub>2</sub>Cl, the anionic and cationic substructure will be discussed separately because of the complex distribution of the mobile silver ions and the resulting highly disordered cation framework. Crystal structures are displayed using the Diamond program package<sup>21</sup> and jpdf plots are visualized by the SCIAN<sup>22</sup> routine.

**Anion Substructure.** The anionic framework of  $\alpha$ -Ag<sub>5</sub>Te<sub>2</sub>Cl can be regarded as a regular 4<sup>4</sup> net composed of chlorine atoms, which is intercalated by a regular 3<sup>2</sup>434 net of tellurium atoms (see Figure 1). These two planar nets are represented by a dashed line and a solid line in Figure 1, respectively.

The structural changes which occur during the two phase transitions manifest themselves in small deviations from the regular arrangement of the two nets. The anionic substructures of all phases are thus related by a group subgroup relation (see Supporting Information). Passing the  $\alpha$ - $\beta$  phase transition, a distortion of the tellurium net occurs in  $\beta$ -Ag<sub>5</sub>Te<sub>2</sub>Cl while the chlorine 4<sup>4</sup> net remains almost unchanged. Looking parallel to the two nets (Figure 2), one can observe a dislocation of tellurium as well as a slight sine-like modulation of the chloride positions in [010] (Figure 2, middle) as compared to the distribution of the anions in  $\alpha$ -Ag<sub>5</sub>Te<sub>2</sub>Cl (Figure 2, top). Both effects are becoming more pronounced while undergoing the second phase transition to end up with  $\gamma$ -Ag<sub>5</sub>Te<sub>2</sub>Cl.

Upon the transformation of  $\beta$ -Ag<sub>5</sub>Te<sub>2</sub>Cl to  $\gamma$ -Ag<sub>5</sub>Te<sub>2</sub>Cl, the ordered 4<sup>4</sup> chloride net disappears and

(20) Freudenthaler, E.; Pfitzner, A. *Solid State Ionics* **1997**, *101*, 1053.

(21) Brandenburg, K. *Diamond, Visualisation package for crystal structures*, ver. 2.1e; Crystal Impact GbR.: Bonn, Germany, 2001.

(22) Pepke, E. *Scian, Visualisation package*, Ver. 1.1; Supercomputer Computation Research Institute, Florida State University: Tallahassee, FL, 1996.

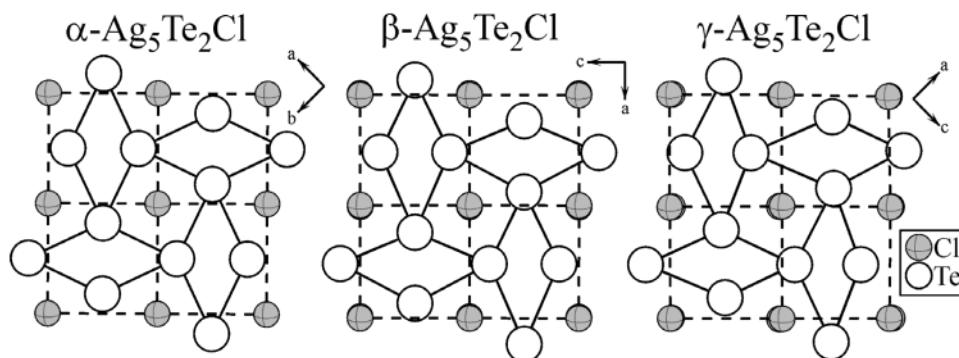


**Figure 1.** Projections of the anion substructures of  $\alpha$ -,  $\beta$ -, and  $\gamma$ - $\text{Ag}_5\text{Te}_2\text{Cl}$ . A regular  $4^4$  (chlorine) and a regular  $3^2 4^3 4$  (tellurium) net distorts while undergoing the phase transitions.

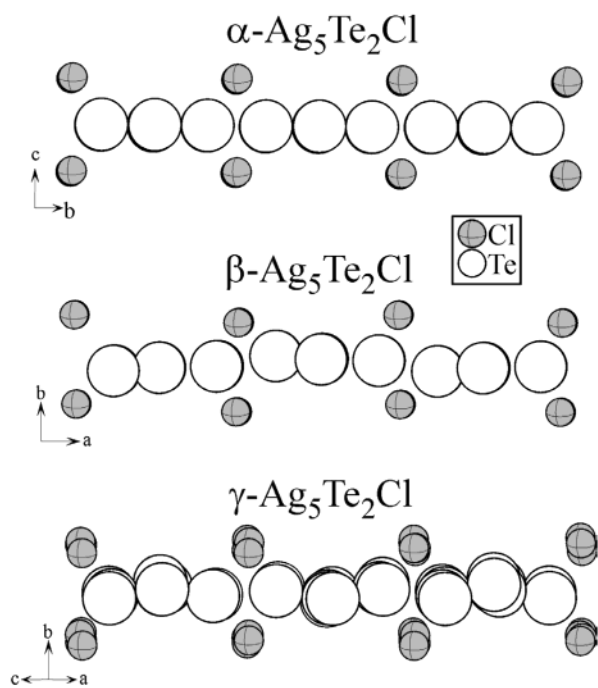


**Figure 2.** Stepwise dislocation of the anion substructure from the  $\alpha$ -phase to the  $\gamma$ -phase of  $\text{Ag}_5\text{Te}_2\text{Cl}$  illustrated by corresponding projections.

the distortion of the tellurium net becomes more obvious. The anionic framework exhibits some similarities to the bismuth substructure of the  $\text{In}_5\text{Bi}_3$  structure type.<sup>8,23–25</sup>

**Cation Substructure.** In contrast to the vivid description of two intercalating networks for the anion substructure, a completely different strategy has to be used to illustrate the cation substructure. The description of the cation substructure by an arrangement of silver clusters has been chosen for the low-temperature phase  $\gamma$ - $\text{Ag}_5\text{Te}_2\text{Cl}$ .<sup>8</sup> In the following we use a more efficient and illustrative way to represent the silver distribution, which is helpful when phase transitions and ordering phenomena occur. We focus on the local environment of the silver atoms and their coordination spheres to highlight the ionic mobility and the arrangement of silver along the diffusion pathways (see jpdf

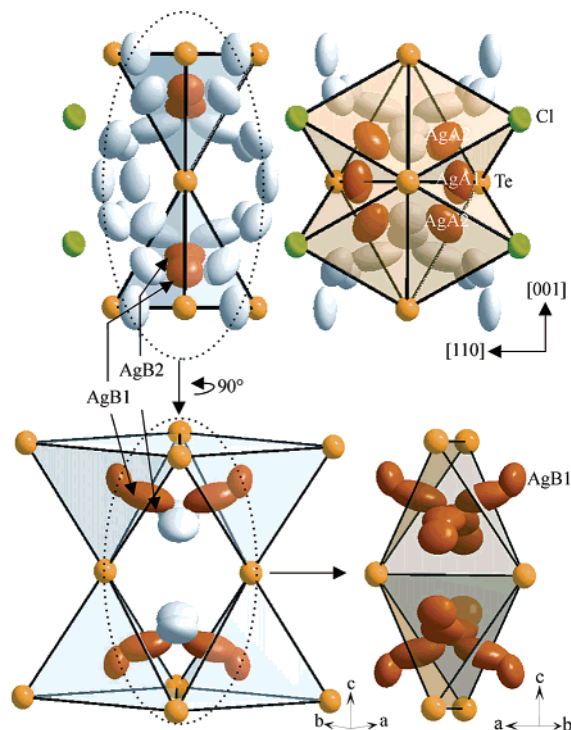


**Figure 3.** Sections of the crystal structure of  $\alpha$ - $\text{Ag}_5\text{Te}_2\text{Cl}$ . Coordination polyhedra formed by the anions around the four silver positions of  $\alpha$ - $\text{Ag}_5\text{Te}_2\text{Cl}$  are shown. Ellipsoids are drawn at a 90% probability level.

analysis and conductivity measurements). To clarify the relation between the silver positions of the different polymorphs, we have defined two groups of silver positions ( $\text{AgA1/A2}$  and  $\text{AgB1/B2}$ ) in  $\alpha$ - $\text{Ag}_5\text{Te}_2\text{Cl}$ . All silver positions of  $\beta$ - or  $\gamma$ - $\text{Ag}_5\text{Te}_2\text{Cl}$  having the same group code (A or B) are related to the corresponding group in  $\alpha$ - $\text{Ag}_5\text{Te}_2\text{Cl}$ .

One can illustrate the silver positions in relation to the anionic substructure by defining two different sets of tetrahedra. One set is formed by three Te and one Cl located around the  $\text{AgA1}$  and  $\text{AgA2}$  positions (see Figure 3). Each tetrahedron is surrounded by two further tetrahedra sharing common Te–Te edges. Four  $[\text{Te}_3\text{Cl}]$  tetrahedra share one common corner.  $\text{AgA2}$  is  $[3 + 1]$  coordinated by Te and Cl. Linearly coordinated  $\text{AgA1}$  (Figure 3, top right) acts as a linker to connect two neighboring  $\text{AgA2}$  positions within these tetrahedra.

A second set of tetrahedra is formed exclusively by Te around the  $\text{AgB1}$  and  $\text{AgB2}$  positions (see Figure 3). The  $\text{AgB1}$ –Te distances vary from 2.83(2) to 3.09(1) Å.

(23) Blachnik, R.; Dreisbach, H. A. *J. Solid State Chem.* **1984**, *52*, 53.

(24) Doert, Th.; Asmuth, R.; Böttcher, P. *J. Alloys Compd.* **1994**, *209*, 151.

(25) Böttcher, P.; Doert, Th.; Druska, Ch.; Brandtmöller, S. *J. Alloys Compd.* **1997**, *246*, 209.

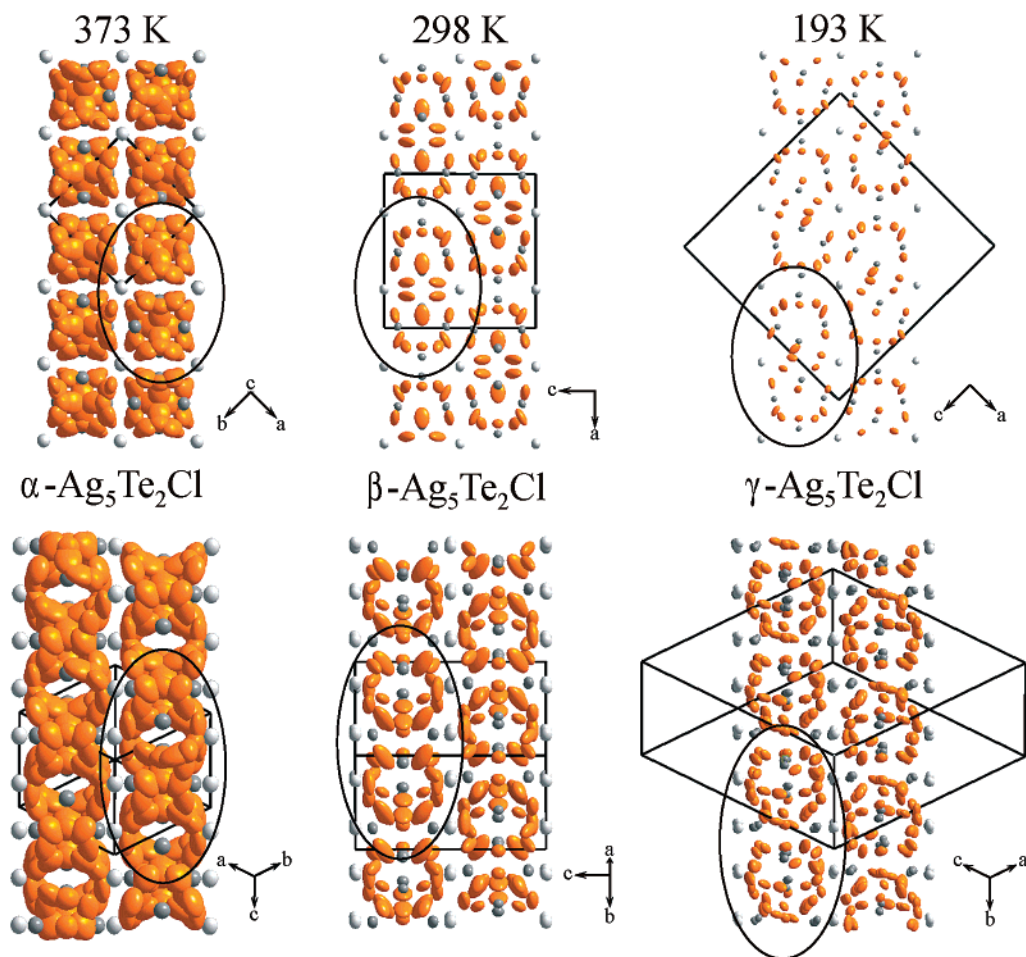


**Figure 4.** Sections of the crystal structures of the  $\alpha$ -,  $\beta$ -, and  $\gamma$ -phase of  $\text{Ag}_5\text{Te}_2\text{Cl}$ . The unit cells are given and corresponding regions in the different phases are marked. The probability level is 90%. Top: Two isolated silver strands in  $\alpha$ - $\text{Ag}_5\text{Te}_2\text{Cl}$  (top left, cords along [001]) are clustering to a double strand in  $\beta$ - and  $\gamma$ - $\text{Ag}_5\text{Te}_2\text{Cl}$ . Bottom:  ${}^{\infty}_{\infty}[\text{Ag}]$  cords of  $\alpha$ - $\text{Ag}_5\text{Te}_2\text{Cl}$  (bottom left) are disintegrated to isolated silver clusters in  $\beta$ - and  $\gamma$ - $\text{Ag}_5\text{Te}_2\text{Cl}$ . Cl, light gray dots; Te, dark gray dots; Ag, brown dots.

These distances are in good agreement with the ones reported for other silver tellurium compounds.<sup>26–28</sup> The shortest distance to the next nearest chlorine atom ( $d(\text{Ag}-\text{Cl}) = 3.90(1) \text{ \AA}$ ) cannot be regarded as a bonding distance. The AgB1 centered  $[\text{Te}_4]$  tetrahedra are linked by a common edge (see Figure 3). Three-coordinate AgB2 is localized on one face of the AgB1 centered  $[\text{Te}_4]$  tetrahedra. A tendency to occupy a double-tetrahedral void close to the AgB1 center can be derived from the displacement parameters of the AgB2 position (Figure 3, bottom right).

AgA1, AgA2, AgB1, and AgB2 are forming 1D endless silver cords (Figure 4, top, view parallel to the cords). All silver positions are only partially occupied.

While the cation substructure of  $\alpha$ - $\text{Ag}_5\text{Te}_2\text{Cl}$  can be regarded as a pseudo molten phase, the cation substructure of  $\beta$ - $\text{Ag}_5\text{Te}_2\text{Cl}$  is more or less ordered. That means that the silver atoms are more or less localized and the distance range of neighboring silver positions is sharpened around a physically meaningful distance ( $d_{\text{min}}(\text{Ag}-\text{Ag}) = 2.769(4) \text{ \AA}$ ). All positions are fully occupied now. Nevertheless, the silver atoms still show large displacement parameters, which leads to the conclusion that

they are still mobile in  $\beta$ - $\text{Ag}_5\text{Te}_2\text{Cl}$ . Compared to the  ${}^{\infty}_{\infty}[\text{Ag}]$  cords of  $\alpha$ - $\text{Ag}_5\text{Te}_2\text{Cl}$ , the distribution of silver atoms changes in  $\beta$ - $\text{Ag}_5\text{Te}_2\text{Cl}$  and  $\gamma$ - $\text{Ag}_5\text{Te}_2\text{Cl}$ . Looking along [001] in  $\alpha$ - $\text{Ag}_5\text{Te}_2\text{Cl}$ , that is, parallel to the cords, it becomes obvious that two silver cords combine to form a single arrangement, Figure 4, top row. The  ${}^{\infty}_{\infty}[\text{Ag}]$  strands are disintegrated to form isolated silver areas during the phase transitions, Figure 4, bottom row.

**jpdf Analysis.** Due to the pronounced disorder of silver atoms over various positions in addition to large atomic displacement parameters resulting in the silver cords discussed above, at least a 1D transport of silver has to be considered. To verify this, the joint probability density function<sup>12,13</sup> (jpfd) of all silver positions has been calculated. Figure 5 shows the jpfd of all silver positions implemented into a projection of the crystal structure of  $\alpha$ - $\text{Ag}_5\text{Te}_2\text{Cl}$ .

It becomes evident that a 1D diffusion path of silver with continuous probability density between the silver positions is present in  $\alpha$ - $\text{Ag}_5\text{Te}_2\text{Cl}$ . The shortest Ag–Ag distance between adjacent cords is found between the AgA2 positions. The jpfd between two AgA2 positions (Figure 6) proves that the probability density is low between the cords, which makes a 3D transport of silver less favorable.

The analyses of the jpfd of  $\beta$ - $\text{Ag}_5\text{Te}_2\text{Cl}$  support the results of the X-ray structure determination. The clus-

(26) Range, K.-J.; Zabel, M.; Rau, F.; von Krziwanek, F.; Marx, R.; Panzer, B. *Angew. Chem.* **1982**, *94*, 717.

(27) Schneider, J.; Schulz, H. *Z. Kristallogr.* **1993**, *203*, 1.

(28) Kaelin, W.; Guenter, J. R. *J. Solid State Chem.* **1996**, *123*, 391.

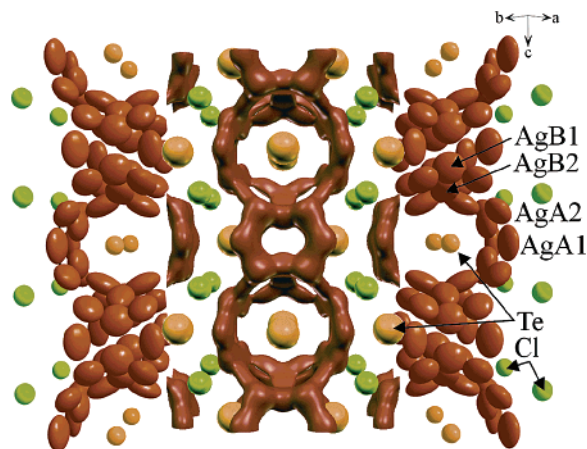


**Figure 5.** Perspective view of the crystal structure of  $\alpha\text{-Ag}_5\text{Te}_2\text{Cl}$  at 373 K. Refined anisotropic positions (left and right cord, probability 50%) and jpdf (middle part, isovalue 0.08) indicating the high mobility of silver at elevated temperatures. A continuous 1D silver diffusion pathway is present in [001].

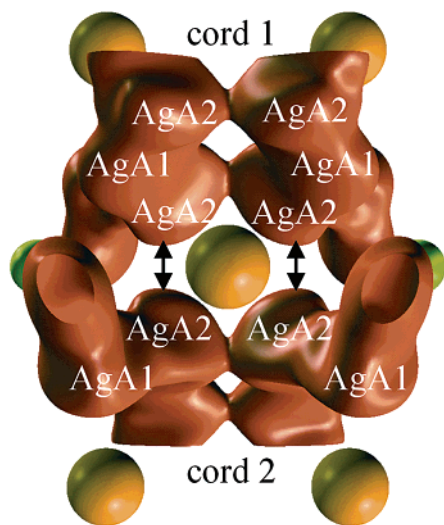


**Figure 6.** jpdf of two neighbored Ag cords of  $\alpha\text{-Ag}_5\text{Te}_2\text{Cl}$ . The closest distance of silver is marked by double arrows. A diffusion path leading to a 3D diffusion of silver can be estimated from the shape of the jpdf. The probability density between the Ag cords is significantly lower than that within the cords.

tering of silver atoms leads to isolated areas of high silver probability density. Within these areas the activation energy for the silver diffusion calculated from one particle potentials (opp)<sup>13,29</sup> is still remarkably low and lies well below the activation energy determined for the bulk phase by impedance spectroscopy. Figure 7 shows a jpdf map and an opp plot of the AgA6 and AgA7 position. An activation energy of approximately 0.26 eV can be found between these positions.

**ac Conductivity Measurements.** The  $\infty[\text{Ag}]$  diffusion pathway of  $\alpha\text{-Ag}_5\text{Te}_2\text{Cl}$  interrupted by regions of low silver probability density is supposed to have consequences on the ionic conductivity. We thus performed a detailed examination of the electrical properties around the  $\alpha\text{-}\beta$  phase transition and a determination of the activation energies for both modifications.

ac plots (Nyquist type) show the typical development for an ionic conductor, that is, a semicircle at high

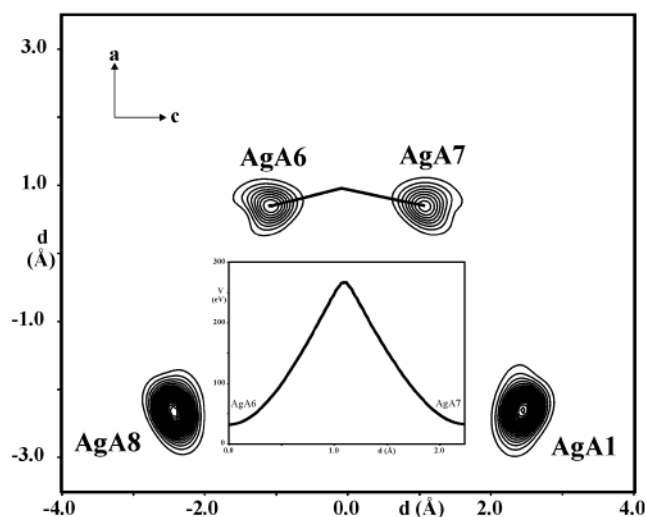


**Figure 7.** jpdf map of  $\text{Ag}_5\text{Te}_2\text{Cl}$  at 298 K incorporating AgA1, AgA8, AgA6, and AgA7. Minimum density  $-0.016 \text{ \AA}^{-3}$ , maximum density  $+4.13 \text{ \AA}^{-3}$ , contour lines  $+0.2 \text{ \AA}^{-3}$ , negative regions omitted. The plane is chosen to maximize the jpdf between AgA6 and AgA7. A line between AgA6 and AgA7 represents the way to calculate the one particle potential (opp).

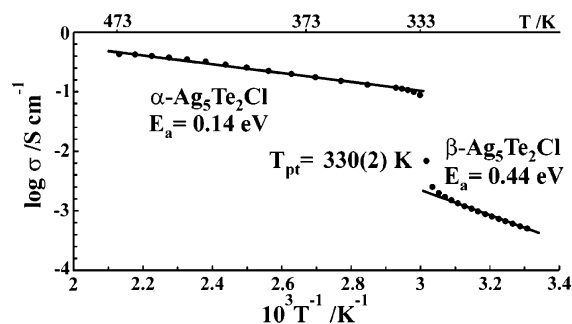


**Figure 8.** Arrhenius plot of the total conductivity of  $\alpha\text{-}$  and  $\beta\text{-Ag}_5\text{Te}_2\text{Cl}$ .

frequencies in addition to a linear spike at low frequencies. The conductivity for  $\beta\text{-Ag}_5\text{Te}_2\text{Cl}$  at 323 K, slightly below the phase transition to the high-temperature form, is  $\sigma = 1.51 \times 10^{-3} \Omega^{-1} \text{ cm}^{-1}$ . At 469 K the conductivity  $\sigma = 4.30 \times 10^{-1} \Omega^{-1} \text{ cm}^{-1}$  of  $\alpha\text{-Ag}_5\text{Te}_2\text{Cl}$  is more than 2 orders of magnitude higher. These data are in good agreement with the observations of Beeken et al.<sup>9</sup> We fitted the measured conductivities versus the reciprocal temperature to determine the activation energies using an Arrhenius-like expression. Figure 8 shows a typical Arrhenius plot of  $\text{Ag}_5\text{Te}_2\text{Cl}$  from which the activation energies of 0.14 eV for  $\alpha\text{-Ag}_5\text{Te}_2\text{Cl}$  and 0.44 eV for  $\beta\text{-Ag}_5\text{Te}_2\text{Cl}$  can be deduced, respectively.

These activation energies differ significantly from those determined by Beeken et al. The activation energy of the high-temperature phase is well below 0.3 eV, which may make it interesting for applications in electrochemical devices.<sup>10</sup> Compared to numerous silver-based ionic conductors such as  $\text{AgI}$ ,  $\text{Ag}_2\text{Q}$  ( $\text{Q} = \text{S}, \text{Se}, \text{Te}$ ) or  $\text{Ag}_3\text{SI}$ ,<sup>10</sup>  $\text{Ag}_5\text{Te}_2\text{Cl}$  has a low transition temperature to its superionic phase in addition to a low activation energy. In contrast to the thermodynamically nonstable phases  $\text{MAG}_4\text{I}_5$  ( $\text{M} = \text{Rb}, \text{K}, \text{NH}_4$ )<sup>1,30</sup> at room-temperature  $\text{Ag}_5\text{Te}_2\text{Cl}$  shows no decomposition in the presence of moisture or light over months. Silver NMR

(29) Kuhs, W. F. *Acta Crystallogr.* **1992**, *A48*, 80.

(30) Topol, L. E.; Owens, B. B. *J. Phys. Chem.* **1968**, *72*, 2106.

spectroscopic investigations<sup>31</sup> performed in the stability area of  $\gamma$ -Ag<sub>5</sub>Te<sub>2</sub>Cl show an activation energy of 0.42 eV, which is supposed to be the same as that for  $\beta$ -Ag<sub>5</sub>Te<sub>2</sub>Cl within the experimental error. This finding corresponds to the data reported earlier where no difference in the activation energies of the  $\beta$ - and  $\gamma$ -phase could be observed.<sup>9</sup>

### Conclusion

Ag<sub>5</sub>Te<sub>2</sub>Cl is a polymorphic material showing two reversible phase transitions at 240.9 and 334.2 K, respectively. The structures and electrical properties of  $\alpha$ -Ag<sub>5</sub>Te<sub>2</sub>Cl and  $\beta$ -Ag<sub>5</sub>Te<sub>2</sub>Cl have been investigated by single-crystal structure analyses and impedance spectroscopy.

The previously unknown structure of  $\beta$ -Ag<sub>5</sub>Te<sub>2</sub>Cl could be determined from single-crystal X-ray diffraction after a special temperature treatment.  $\beta$ -Ag<sub>5</sub>Te<sub>2</sub>Cl has to be regarded as an intermediate polymorph between the silver ion conductor  $\alpha$ -Ag<sub>5</sub>Te<sub>2</sub>Cl and  $\gamma$ -Ag<sub>5</sub>Te<sub>2</sub>Cl with a complete ordering of the silver atoms. All three polymorphs are closely related by symmetry and systematic twinning occurs during the transition from the  $\alpha$ - to the  $\beta$ -phase. On the basis of a modified structure model, a jpdf analysis of the diffusion pathways was performed for  $\alpha$ -Ag<sub>5</sub>Te<sub>2</sub>Cl and  $\beta$ -Ag<sub>5</sub>Te<sub>2</sub>Cl.

$\alpha$ -Ag<sub>5</sub>Te<sub>2</sub>Cl is an interesting ion conductor with a conductivity and an activation energy comparable to

AgI, RbAg<sub>4</sub>I<sub>5</sub>, or Ag<sub>3</sub>SI. A pronounced one-dimensional mobility of silver along [001] can be estimated from jpdf analysis and anisotropic conduction behavior seems probable. Further examinations which prove this assumption are still in progress.

Large displacement parameters and low activation energies between selected silver positions indicate that a certain mobility of the silver ions is still present in  $\beta$ -Ag<sub>5</sub>Te<sub>2</sub>Cl and the conductivity of about  $10^{-3} \Omega^{-1} \text{cm}^{-1}$  for this phase still is remarkably high.

**Acknowledgment.** We thank Prof. T. Fässler, TH Darmstadt, and Stoe & Cie GmbH, Darmstadt, for the possibility to use the IPDS II and high-temperature device and the DFG and the Fonds der Chemischen Industrie for financial support.

**Supporting Information Available:** Tables of atomic coordinates, bond lengths and angles, and anisotropic displacement parameters of  $\beta$ - and  $\alpha$ -Ag<sub>5</sub>Te<sub>2</sub>Cl (PDF, CIF); powder diffraction data and group-subgroup relations (PDF). This material is available free of charge via the Internet at <http://pubs.asc.org>. Further details of the crystal structure investigations are available from the Fachinformationszentrum Karlsruhe, D-76334 Leopoldshafen (Germany), fax 0049 7247 808 666, email [crysdata@fiz-karlsruhe.de](mailto:crysdata@fiz-karlsruhe.de), on quoting the depository numbers CSD-413506 ( $\alpha$ , 373 K), -413507 ( $\alpha$ , 423 K), -513508 ( $\alpha$ , 543 K), -413510 ( $\beta$  crystal 1, 298 K), -413509 ( $\beta$  crystal 2, 298 K), the name of the authors, and the reference of the publication.

CM031131C

(31) Nilges, T.; Pfitzner, A.; Doert, T.; Brinkmann, C.; Vogel, M.; Eckert, H. Unpublished results, 2003.